**Proceedings of the 17th World Congress**
**The International Federation of Automatic Control**
**Seoul, Korea, July 6-11, 2008**

# Solving the Goddard problem with thrust and dynamic pressure constraints using saturation functions

**Knut Graichen Nicolas Petit**

*Centre Automatique et Systèmes, Ecole des Mines de Paris,*
*75272 Paris, France (e-mail: {knut.graichen , nicolas.petit}@ensmp.fr)*

**Abstract:** This paper addresses the well-known Goddard problem in the formulation of Seywald and Cliff with the objective to maximize the altitude of a vertically ascending rocket subject to dynamic pressure and thrust constraints. The Goddard problem is used to propose a new method to systematically incorporate the constraints into the system dynamics by means of saturation functions. This procedure results in an unconstrained and penalized optimal control problem which strictly satisfies the constraints. The approach requires no knowledge of the switching structure of the optimal solution and avoids the explicit consideration of singular arcs. A collocation method is used to solve the BVPs derived from the optimality conditions and demonstrates the applicability of the method to constrained optimal control problems.

Keywords: Optimal control; State and input constraints; Two–point boundary value problem; Aerospace applications.

## 1. INTRODUCTION

The classical Goddard problem presented in 1919 (Goddard, 1919) concerns maximizing the final altitude of a rocket launched in vertical direction. The problem has become a benchmark example in optimal control due to a characteristic singular arc behavior in connection with a relatively simple model structure, which makes the Goddard rocket an ideal object of study, see e.g. (Garfinkel, 1963; Munick, 1965; Tsiotras and Kelley, 1992; Seywald, 1994; Bryson, 1999; Milam, 2003).

A particularly interesting formulation of the Goddard problem is given by Seywald and Cliff (Seywald and Cliff, 1992), who considered both thrust and dynamic pressure constraints. This significantly complicates the Goddard problem, since the dynamic pressure constraint represents a first–order state constraint (in the sense of (Bryson and Ho, 1969, Ch. 3.11)) in addition to the "zeroth–order" thrust constraint. Based on Pontryagin's maximum principle, Seywald and Cliff thorougly investigated the singular arcs and the optimal switching structure of the system. The analytical effort which is required to consider the constraints and singular arcs of the Goddard problem is a well–known difficulty with constrained OCPs. In particular, the switching structure of the optimal solution must be known a–priori and leads to interior boundary conditions for the boundary value problem (BVP) derived from the optimality conditions (Bryson and Ho, 1969).

In this contribution, the Goddard problem with thrust and dynamic pressure constraints (Seywald and Cliff, 1992) is used as an example to present a new method for handling constraints in optimal control by means of saturation functions. Following the ideas in (Graichen, 2006) originally developed in the context of feedforward control design, the saturation function approach takes advantage of the fact that the thrust and dynamic pressure constraints have different orders. The saturation functions are used to successively incorporate the constraints within a new system representation, which strictly satisfies the constraints. In this way, the original constrained optimal control problem (OCP) is replaced by an unconstrained one, which can be treated by the standard calculus of variations without requiring knowledge of the switching structure of the optimal solution. An additional penalty term is introduced in the cost of the derived unconstrained OCP to avoid singular arcs, which correspond to active constraints in the original constrained OCP. The penalty term has the positive side effect that the original singular arcs in the Goddard problem are circumvented.

The differential–algebraic equations of the BVP stemming from the optimality conditions are numerically solved with a modified version of the collocation–based BVP solver bvp4c of Matlab. The penalty term in the BVP is thereby continuously decreased in order to approach the optimal solution of the Goddard problem.

The paper is organized as follows: Section 2 summarizes the Goddard problem with the thrust and dynamic pressure constraints. Section 3 describes in a first step the incorporation of the thrust constraint in order to illustrate the idea of the saturation function approach. Section 4 describes the collocation method for the solution of the BVP derived from the optimality conditions and presents the numerical results for the thrust–constrained Goddard problem. Section 5 is devoted to the additional incorporation of the dynamic pressure constraint by means of the saturation functions. The numerical results for the Goddard problem with thrust and dynamic pressure constraints show the applicability of the approach as well as the accuracy of the employed collocation method. It represents a first step in the development towards a general methodology to efficiently solve constrained optimal trajectory generation problems.

## 2. PROBLEM FORMULATION

The Goddard problem is to maximize the final altitude of a vertically ascending rocket under the influence of atmospheric drag and the gravitational field. This section shortly summarizes the equations of motion of the rocket as well as the boundary conditions and constraints of the corresponding OCP.

### *2.1 Model equations*

The equations of motion of the rocket are given by the ordinary differential equations (ODEs)

$$\dot{h} = v\,, \tag{1a}$$

$$\dot{v} = \frac{u - D(h,v)}{m} - \frac{1}{h^2}\,, \tag{1b}$$

$$\dot{m} = -\frac{u}{c} \tag{1c}$$

with the altitude $h$ from the center of Earth, the velocity $v$, and the mass $m$ as the mass of the rocket (Seywald and Cliff, 1992; Bryson, 1999). The states $h$, $v$, $m$, the thrust $u$ as the input of the system, and the time $t$ are commonly normalized and dimension–free.

The drag function $D(h,v)$ in (1b) is given by

$$D(h,v) = q(h,v)\frac{C_D A}{m_0 g} \tag{2}$$

as a function of the Earth's gravitational acceleration $g$ and the dynamic pressure

$$q(h,v) = \frac{1}{2}\,\rho_0\, v^2 \exp\Big(\beta(1-h)\Big) \tag{3}$$

that depends on the altitude $h$ and the velocity $v$. The constants in the model equations (1)–(3) are

| | | | |
|---|---|---|---|
| $C_D$ | drag coefficient, | $\rho_0$ | air density at sea level, |
| $A$ | reference area, | $\beta$ | density decay rate, |
| $m_0$ | initial mass, | $c$ | exhaust velocity. |

The following values are taken from (Seywald and Cliff, 1992):

$$\beta = 500\,, \quad c = 0.5\,, \quad \frac{\rho_0 C_D A}{m_0 g} = 620\,.$$

### *2.2 Constraints and boundary conditions*

The (normalized) thrust as the control of the rocket is subject to the constraint

$$u \in [u^-, u^+], \quad u^- = 0, \quad u^+ = 3.5\,. \tag{4}$$

In addition, Seywald and Cliff (1992) considered a constraint on the dynamic pressure (3)

$$q(h,v) \le q^+, \quad q^+ = 1\,, \tag{5}$$

which can be interpreted as a first–order state constraint for the velocity $v$ of the rocket. This point will be explained in more detail in Section 5.

The rocket starts at the Earth's surface and is initially at rest. This yields the normalized initial conditions

$$h(0) = 1\,, \quad v(0) = 0\,, \quad m(0) = 1\,. \tag{6}$$

The only final condition at the free final time $T$ is imposed on the mass

$$m(T) = 0.6 \tag{7}$$

to account for the consumed fuel of the rocket with respect to its initial mass.

In its original formulation, the objective of the Goddard problem is to maximize the final altitude $h(T)$. Hence, the constrained optimal control problem is to minimize the cost

$$J = -h(T) \tag{8}$$

with the unknown end time $T$ subject to the system dynamics (1), the constraints (4), (5), and the boundary conditions (6), (7).

## 3. CONSIDERATION OF THRUST CONSTRAINT

This constrained OCP of the Goddard rocket can be solved with Pontryagin's maximum principle. However, the consideration of the constraints (4), (5) and the singular arcs of the Goddard problem require to analytically investigate the switching structure of the optimal solution and lead to interior boundary conditions (Seywald and Cliff, 1992).

A different way to systematically incorporate the constraints within the system is by means of saturation functions (Graichen, 2006). In a first step, this section considers the input constraint (4) in order to introduce the idea of the saturation function approach.

### *3.1 Asymptotic saturation function*

The input constraint (4) can be incorporated by replacing the input $u$ with a monotonically increasing saturation function

$$u = \psi(\tilde{u}, \psi^{\pm})\,, \tag{9a}$$

which represents a surjective mapping $\mathbb{R} \ni \tilde{u} \mapsto \psi(\tilde{u}, \psi^{\pm}) \in (\psi^-, \psi^+)$ of the new unconstrained input $\tilde{u}$. The saturation limits $\psi^-$ and $\psi^+$ (in compact form $\psi^{\pm}$) directly correspond to (4), i.e.

$$\psi^{\pm} = u^{\pm}, \tag{9b}$$

where it is assumed that $\psi^-$ and $\psi^+$ are asymptotically reached for $\tilde{u} \to \pm\infty$, see Fig. 1.

An appropriate choice for $\psi(\tilde{u}, \psi^{\pm})$ is e.g.

$$\psi(\tilde{u}, \psi^{\pm}) = \psi^+ - \frac{\psi^+ - \psi^-}{1 + \exp(s\,\tilde{u})}\,. \tag{10}$$

The parameter $s$ is chosen to

$$s = \frac{4}{\psi^+ - \psi^-}$$

in order to normalize the slope $\partial\psi/\partial\tilde{u} = 1$ at $\tilde{u} = 0$. Alternatively, tanh–functions could be used instead of (10).

The saturation function (9a) replaces the input $u$ in the model (1), which yields the modified dynamics

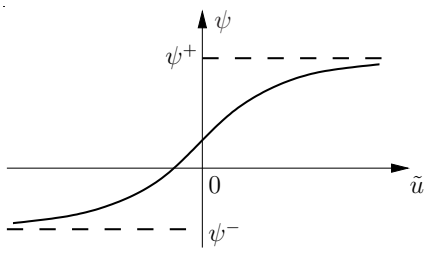


Fig. 1. Saturation function $\psi(\tilde{u}, \psi^{\pm}) \in (\psi^-, \psi^+)$.

$$\dot{h} = v\,, \tag{11a}$$
$$\dot{v} = \frac{\psi(\tilde{u},\psi^{\pm}) - D(h,v)}{m} - \frac{1}{h^2}\,, \tag{11b}$$
$$\dot{m} = -\frac{\psi(\tilde{u},\psi^{\pm})}{c}\,. \tag{11c}$$

with the new unconstrained input $\tilde{u}$.

### 3.2 Necessary optimality conditions

In order to derive the optimality conditions for the transformed model (11) by means of the calculus of variations, the cost (8) to be minimized is penalized by

$$J_\varepsilon = -h(T) + \frac{\varepsilon}{2}\int_0^T \tilde{u}^2\,\mathrm{d}t\,, \tag{12}$$

subject to the modified system dynamics (11) and the boundary conditions (6), (7) written in the general nonlinear form

$$\dot{x} = f(x,\tilde{u}), \quad x(0) = (1,0,1)^{\mathsf{T}}, \quad x_3(T) = 0.6\,. \tag{13}$$

The additional penalty term in (12) with parameter $\varepsilon$ is necessary to account for the influence of the saturation close to the constraints (4). This point can be explained by considering the Hamiltonian

$$H(x,\lambda,\tilde{u},t) = \frac{\varepsilon}{2}\,\tilde{u}^2 + \lambda^{\mathsf{T}} f(x,\tilde{u})$$

and the optimality condition $\partial H/\partial\tilde{u} = 0$ with respect to the new input $\tilde{u}$:

$$\frac{\partial H}{\partial \tilde{u}} = \varepsilon\,\tilde{u} + \lambda^{\mathsf{T}}\frac{\partial f}{\partial \tilde{u}} = \varepsilon\,\tilde{u} + \frac{\partial \psi}{\partial \tilde{u}}\left(\frac{\lambda_2}{m} - \frac{\lambda_3}{c}\right) = 0\,. \tag{14}$$

If the saturation function $\psi(\tilde{u},\psi^{\pm})$ approaches one of its limits $\psi^{\pm}$, i.e. the input constraint (4) is almost active, the gradient $\partial\psi/\partial\tilde{u}$ will tend to zero, cf. Fig. 1. Hence, the penalty term $\varepsilon\,\tilde{u}$ in (14) is introduced to still be able to determine the new input $\tilde{u}$ from (14) if the gradient $\partial\psi/\partial\tilde{u}$ vanishes close to saturation.

To complete the optimality conditions, the adjoint state $\lambda = (\lambda_1,\lambda_2,\lambda_3)^{\mathsf{T}}$ is given by $\dot{\lambda}^{\mathsf{T}} = -\partial H/\partial x$ with

$$\begin{aligned}
\dot{\lambda}_1 &= \frac{\lambda_2}{m}\frac{\partial D}{\partial h} - \lambda_2\frac{2}{h^3} && \lambda_1(T) = 0\,,\\
\dot{\lambda}_2 &= \frac{\lambda_2}{m}\frac{D}{v} - \lambda_1, && \lambda_2(T) = 0\,,\\
\dot{\lambda}_3 &= \frac{\lambda_2}{m^2}\Big(\psi(\tilde{u},\psi^{\pm}) - D(h,v)\Big), && \lambda_3(T) = free.
\end{aligned} \tag{15}$$

The free end time $T$ is taken into account by the transversality condition

$$H(x,\lambda,\tilde{u},t)\big|_{t=T} = 0\,. \tag{16}$$

The systems (13) and (15) with the additional final condition (16) and the algebraic equation (14) form a two–point BVP for the penalized OCP of the thrust–constrained rocket in dependence of the parameter $\varepsilon$. The optimal solution can be approached by using a continuation scheme to successively decrease the penalty parameter $\varepsilon \to 0$.

## 4. NUMERICAL SOLUTION WITH COLLOCATION

A powerful method to numerically solve the two–point BVP resulting from the optimality conditions is *collocation* (Ascher et al., 1988). Compared to shooting or gradient algorithms, the collocation method has advantages in handling final conditions and the inherently unstable process of system and adjoint equations (13), (15). [1] This section gives a short overview on the employed collocation method before the numerical results for the Goddard problem with thrust constraints are presented.

### 4.1 Collocation method

The basis for the numerical solution of the reentry problem is the standard MATLAB BVP solver bvp4c, which solves nonlinear 2–point BVPs by means of the collocation method (Shampine et al., 2000). However, to be applicable to optimal control problems, the bvp4c–code was adapted by the authors to additionally account for algebraic equations like (14) as they arise from the optimality conditions. This leads to the general BVP formulation of (index 1) differential–algebraic equations (DAE)

$$\dot{y} = f(y,z,t,p), \tag{17a}$$
$$0 = g(y,z,t,p)\,, \tag{17b}$$
$$0 = h(y(t_0),y(t_f),z(t_0),z(t_f),p) \tag{17c}$$

with the differential and algebraic equations (17a), (17b) for the dynamic and algebraic states $y(t), z(t)$ on the time interval $t \in [t_0,t_f]$, and the boundary conditions (17c). Moreover, unknown parameters $p$ can additionally be considered in the DAE formulation (17).

The general collocation method and its implementation in bvp4c has been left unchanged as it was designed to be applicable and numerically robust for a wide range of BVPs. The function bvp4c divides the time interval $[t_0,t_f]$ in subintervals and discretizes the differential equations (17a) along the time mesh. The resulting discretized system equations together with the boundary conditions (17c) and the additional algebraic equations (17b) evaluated at the mesh points results in a set of nonlinear algebraic equations, which is solved with a Newton iteration scheme.

In addition, bvp4c employs a robust mesh refinement strategy to adapt the time mesh and the number of grid points in each Newton step based on the residual along the discretized ODEs (17a).

### 4.2 Numerical results

In order to apply the collocation method to the Goddard problem, the BVP (13)–(16) has to be adapted to the DAE form (17). The ODEs (17a) are given by the original and adjoint systems in (13) and (15) for the overall dynamic state $y = (x,\lambda)$. The input $u$ denotes the algebraic variable $z = u$ with the algebraic equation (14) corresponding to (17b). The boundary conditions for $x$ and $\lambda$ in (13) and (15) together with the transversality condition (16) are comprised in (17c). The free end time $T$ is taken into account by means of the time transformation

$$t = \delta\tau, \qquad T = \delta, \qquad \frac{\mathrm{d}}{\mathrm{d}t} = \frac{1}{\delta}\frac{\mathrm{d}}{\mathrm{d}\tau} \tag{18}$$

with the normalized time coordinate $\tau \in [0,1]$. Hence, the scaling factor $\delta$ is treated as free parameter $p = \delta$ in the DAE system (17) and the new time coordinate $\tau$ replaces

[1] More information on the numerical solution of OCPs can e.g. be found in the text books (Bryson and Ho, 1969; Bryson, 1999; Pytlak, 1999). A detailed analysis of the collocation method is given in (Ascher et al., 1988).

$t \in [t_0, t_f]$ with the normalized interval boundaries $t_0 = 0$ and $t_f = 1$.

The initial guess for the state $x(t)$ is a linear interpolation between the boundary conditions in (13) and $x_1(T) = x_2(T) = 0$ for the unspecified final states. The initial trajectories for $\lambda(t)$ and $\tilde{u}(t)$ are zero. The free parameter $\varepsilon$ accounting for the unknown end time $T$ is chosen to $\varepsilon = 0.1$.

Fig. 2 shows the optimal trajectories of the states $x(t)$ and dynamic pressure $q(t)$ as well as the original control $u(t)$ for the Goddard problem with different penalty parameters $\varepsilon$ by solving the BVP (13)–(16) with the collocation method and successively decreasing the penalty parameter $\varepsilon$ from $10^{-2}$ to $10^{-11}$. After the initial run with $\varepsilon = 10^{-2}$, the subsequent runs use the previous solutions as initialization. The maximal altitude $h(T)$ and the end time $T$ obtained for $\varepsilon = 10^{-11}$ are (both normalized values)

$$h(T) = 1.01283692, \quad T = 0.19885626\,. \tag{19}$$

Moreover, the final run with $\varepsilon = 10^{-11}$ clearly shows the characteristic bang–singular–bang behavior of the Goddard problem and in particular the sharp flanks in the control $u(t)$, which are accurately obtained due to the automatic mesh refinement strategy.

## 5. CONSIDERATION OF DYNAMIC PRESSURE CONSTRAINT

To show the flexibility of the method, a further constraint of engineering interest is considered. In addition to the thrust constraint (4), the saturation functions can also be used to systematically incorporate the dynamic pressure constraint (5) by following the ideas given in (Graichen, 2006). A requirement for the incorporation of both constraints is that they have distinct orders in order to be "differentially separatable". This condition is indeed satisfied since the dynamic pressure constraint (5) denotes a first–order state constraint compared to the thrust constraint (4) of zeroth–order.

### *5.1 Interpretation of constraints*

The saturation function approach in (Graichen, 2006) was developed in the context of feedforward control design to incorporate constraints on a system output and a finite number of its time derivatives within a new system representation.

This method can be applied to the Goddard problem by interpreting the dynamic pressure constraint (5) as the velocity constraint

$$v \leq v^+, \quad v^+(h) = \sqrt{\frac{2q^+}{\rho_0 \exp\big(\beta(1-h)\big)}}\,. \tag{20}$$

Note that $v^+(h)$ is not constant but depends on the altitude $h$. Moreover, a closer look at the ODE (1b) reveals that the thrust constraint (4) can be mapped to the acceleration

$$\dot{v} \in [\dot{v}^-, \dot{v}^+], \quad \dot{v}^\pm(h,v,m) = \frac{u^\pm - D(h,v)}{m} - \frac{1}{h^2} \tag{21}$$

depending on the states $h$, $v$, and $m$. In this way, the dynamic pressure and thrust constraints are considered as constraints on the velocity $v$ and its time derivative $\dot{v}$.

### *5.2 Systematic incorporation with saturation functions*

In a first step, a saturation function is introduced for the velocity

$$v = \psi_1(\xi, \psi_1^\pm) \tag{22a}$$

with the new unconstrained coordinate $\xi$ and the saturation limits following from (20) [2]

$$\psi_1^\pm(h) = \pm v^+(h)\,. \tag{22b}$$

Again, the saturation function $\psi_1(\xi, \psi_1^\pm)$ can be constructed according to (10), also see Fig. 1. An important point in the following is that the saturation limits $\psi_1^\pm(h)$ are asymptotically reached with $\psi_1(\xi, \psi_1^\pm)$ being strictly monotonically increasing, i.e.

$$\frac{\partial \psi_1}{\partial \xi} > 0 \quad \forall\, \xi \in \mathbb{R}\,. \tag{23}$$

In a next step, Eq. (22a) is differentiated using the product and chain rules and (20), (22b):

$$\dot{v} = \underbrace{\left( \frac{\partial \psi_1}{\partial \psi_1^+} \frac{\partial v^+}{\partial h} - \frac{\partial \psi_1}{\partial \psi_1^-} \frac{\partial v^+}{\partial h} \right) \tilde{\psi}_1(h,\xi)}_{=\,\gamma(h,\xi)} + \frac{\partial \psi_1}{\partial \xi}\,\dot{\xi} \tag{24}$$

with

$$\tilde{\psi}_1(h,\xi) = \psi_1\left(\xi, \psi_1^\pm(h)\right)\,.$$

A second saturation function

$$\dot{\xi} = \psi_2(\tilde{u}, \psi_2^\pm) \tag{25a}$$

is introduced for $\dot{\xi}$ with the new unconstrained input $\tilde{u}$. The saturation limits $\psi_2^\pm$ have to be chosen appropriately such that the relation (24) for $\dot{v}$ satisfies the constraint (21). In view of (24) and (25a), the inequality $\dot{v}^- \leq \dot{v} \leq \dot{v}^+$ can be formulated as

$$\dot{v}^- - \gamma(h,\xi) \;\leq\; \frac{\partial \psi_1}{\partial \xi} \psi_2(\tilde{u}, \psi_2^\pm) \;\leq\; \dot{v}^+ - \gamma(h,\xi)$$

The strict monotonicity assumption (23) allows to divide the term $\partial\psi_1/\partial\xi$ on both sides of the inequality, which yields the following saturation limits for $\psi_2^- < \psi_2(\tilde{u}, \psi_2^\pm) < \psi_2^+$:

$$\psi_2^\pm(h,\xi,m) = \frac{\dot{\tilde{v}}^\pm(h,\xi,m) - \gamma(h,\xi)}{\dfrac{\partial \psi_1}{\partial \xi}} \tag{25b}$$

with the velocity constraints $\dot{\tilde{v}}^\pm(h,\xi,m) = \dot{v}^\pm(h,v,m)$ due to (22).

### *5.3 New system representation*

The result of successively introducing the saturation functions is that the velocity $v$ and ODE (1b) are replaced by (22) with the new coordinate $\xi$ and the corresponding ODE (25). Moreover, the input $u$ of the original system (1) has to be expressed in terms of the new input $\tilde{u}$. This is done by solving the ODE (1b) for $u$ and replacing $v$ and $\dot{v}$ with (22), (24), and (25), i.e.

$$\begin{aligned} u &= m\left( \gamma(h,\xi) + \frac{\partial \psi_1}{\partial \xi} \tilde{\psi}_2(h,\xi,m,\tilde{u}) + \frac{1}{h^2} \right) + \tilde{D}(h,\xi) \\ &= \phi(h,\xi,m,\tilde{u}) \end{aligned} \tag{26}$$

[2] Since $v$ is only constrained from above, the lower saturation limit $\psi_1^-$ is set to $\psi_1^- = -v^+(h)$ for the sake of symmetry.

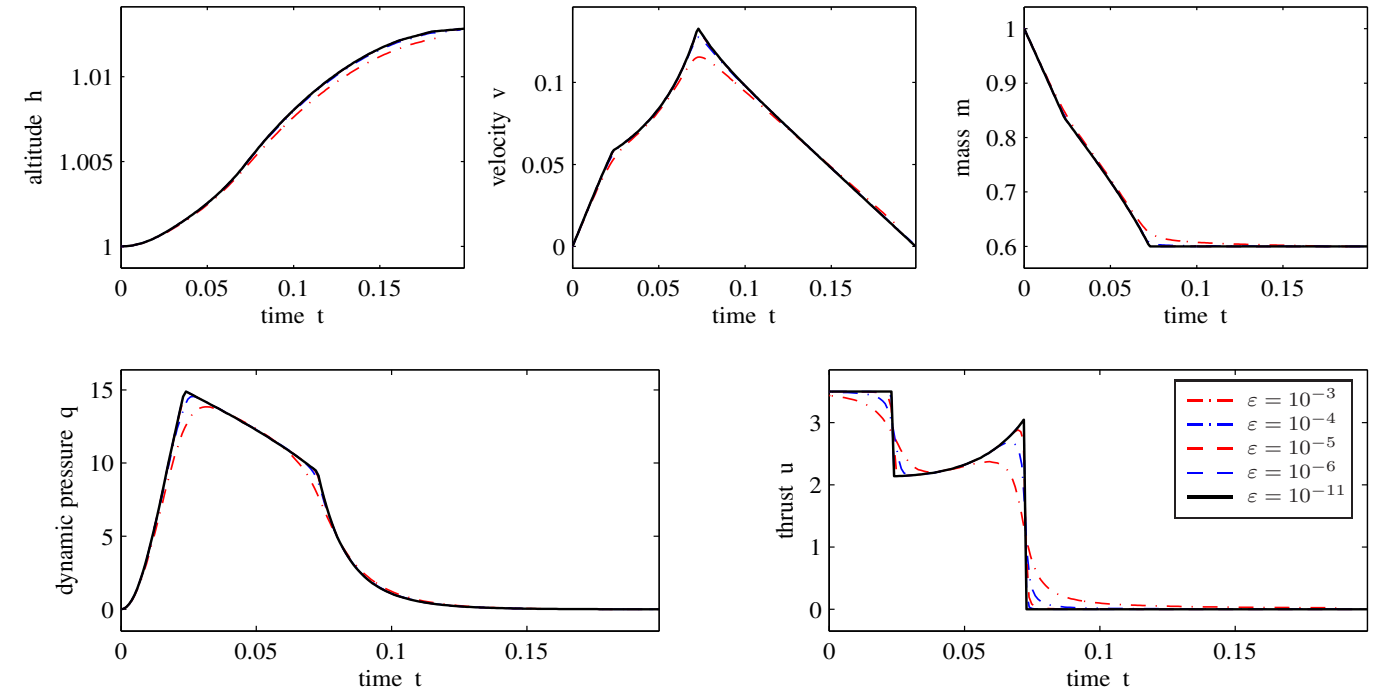


Fig. 2. Optimal trajectories of the Goddard problem with thrust constraints for decreasing penalty parameters $\varepsilon$.

with the compact form

$$\tilde{\psi}_2(h, \xi, m, \tilde{u}) = \psi_2\left(\tilde{u}, \psi_2^{\pm}(h, \xi, m)\right)$$

of the second saturation function. As a result, the original system (1) with the state $x = (h, v, m)^\mathsf{T}$ and input $u$ is replaced by the new system

$$\dot{h} = \tilde{\psi}_1(h, \xi)\,, \tag{27a}$$

$$\dot{\xi} = \tilde{\psi}_2(h, \xi, m, \tilde{u})\,, \tag{27b}$$

$$\dot{m} = -\phi(h, \xi, m, \tilde{u})/c \tag{27c}$$

with the state $\tilde{x} = (h, \xi, m)^\mathsf{T}$ and input $\tilde{u}$. The velocity $v$ and the thrust $u$ follow from the algebraic equations (22) and (26), whereby the saturation functions ensure that the thrust and dynamic pressure constraints (4), (5) are satisfied via the velocity constraints (20), (21).

### *5.4 Necessary optimality conditions*

The derivation of the optimality conditions for the new system (27) corresponds to the input–constrained case in Section 3.2 and is therefore not repeated in detail. The cost (8) to be minimized

$$\tilde{J}_\varepsilon = -h(T) + \frac{\varepsilon}{2}\int_0^T \tilde{u}^2\,\mathrm{d}t\,, \tag{28}$$

is again penalized by the integrated term $\frac{\varepsilon}{2}\tilde{u}^2$ in order to account for the influence of the saturation close to the velocity constraints (20) and (21), see Section 3.2.

The new system dynamics (27) are written in the compact form

$$\dot{\tilde{x}} = \tilde{f}(\tilde{x}, \tilde{u}), \quad \tilde{x}(0) = (1,\, \xi_0, 1)^\mathsf{T}, \quad x_3(T) = 0.6 \tag{29}$$

with the boundary conditions for $\tilde{x}_1 = h$ and $\tilde{x}_3 = m$ following from (6), (7). The initial value $\tilde{x}_2(0) = \xi(0) = \xi_0$ is obtained by inverting the saturation function (22) with respect to $\xi$:

$$\xi_0 = \psi_1^{-1}\left(v(0), \psi_1^{\pm}\right).$$

Since the saturation limits (22b) are symmetric, the saturation function (22a) passes through zero, i.e. $0 = \psi_1(0, \psi_1^{\pm})$, and the initial zero velocity $v(0) = 0$ directly yields $\xi_0 = 0$.

With the Hamiltonian

$$\tilde{H}(x, \tilde{\lambda}, \tilde{u}, t) = \frac{\varepsilon}{2}\tilde{u}^2 + \tilde{\lambda}^\mathsf{T}\tilde{f}(\tilde{x}, \tilde{u})\,,$$

the optimality conditions follow to

$$\frac{\partial \tilde{H}}{\partial \tilde{u}} = \varepsilon\,\tilde{u} + \tilde{\lambda}^\mathsf{T}\frac{\partial \tilde{f}}{\partial \tilde{u}} = 0 \tag{30}$$

$$\dot{\tilde{\lambda}}^\mathsf{T} = -\frac{\partial \tilde{H}}{\partial \tilde{x}} = -\lambda^\mathsf{T}\frac{\partial \tilde{f}}{\partial \tilde{x}}\,, \quad \tilde{\lambda}(T) = (\,0,\, 0,\, \mathit{free}\,)^\mathsf{T} \tag{31}$$

with the additional transversality condition

$$\tilde{H}(\tilde{x}, \tilde{\lambda}, \tilde{u}, t)\big|_{t=T} = 0\,. \tag{32}$$

### *5.5 Numerical results*

The BVP of (index 1) DAEs (29)–(32) for the states $\tilde{x}(t)$, $\tilde{\lambda}(t)$, the new input $\tilde{u}(t)$, and the free end time $T$ is solved with the collocation method described in Section 4. Eventually, the computed trajectories $\tilde{x}(t)$ and $\tilde{u}(t)$ yield the velocity $v(t)$ and the thrust $u(t)$ by evaluating (22) and (26). The initial guess for the trajectories $\tilde{x}(t)$ and $\tilde{u}(t)$ is identical to the thrust–constrained case in Section 4.

Fig. 3 shows the optimal trajectories of the states $x(t)$ and dynamic pressure $q(t)$ as well as the optimal thrust $u(t)$ for the Goddard problem with thrust and dynamic pressure constraints and several penalty parameters $\varepsilon$, which are successively decreased from $10^{-2}$ to $10^{-11}$. The trajectories of the dynamic pressure $q(t)$ and the thrust $u(t)$ clearly stay inside the constraints and show the singular arc behavior of the Goddard problem. The maximum altitude $h(T)$ and the end time $T$ for $\varepsilon = 10^{-11}$ are (both normalized values)

$$h(T) = 1.01271727, \quad T = 0.20407108\,. \tag{33}$$

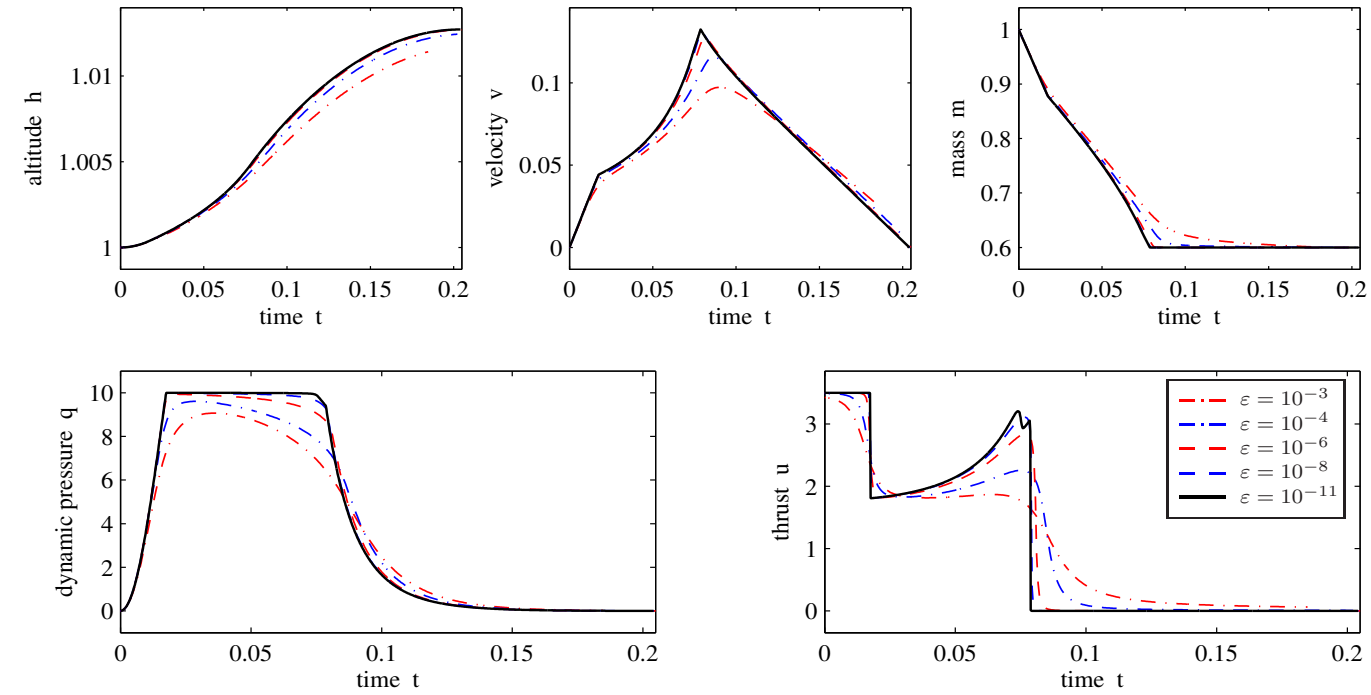


Fig. 3. Optimal trajectories with thrust and dynamic pressure constraints for decreasing penalty parameters $\varepsilon$.

Particularly interesting is the additional singular arc of the thrust $u(t)$ appearing at $t \approx 0.075$, which is due to the additional dynamic pressure constraint. This instance is explained in more details by Seywald and Cliff (1992). Although the singular arc at $t \approx 0.075$ only appears for penalty parameters $\varepsilon < 10^{-10}$ and barely influences the final cost, it shows the applicability of the saturation function approach and the accuracy of the collocation method for solving the BVP (29)–(32).

## 6. CONCLUSIONS

This paper presents a first step towards a new methodology for solving constrained optimal control problems. The Goddard problem with dynamic pressure and thrust constraints serves as a motivating benchmark example, which has been used by numerous authors. Due to the presence of singular arcs and non–intuitive solutions, it stresses the relevance of the new approach, which uses saturation functions to replace the constrained quantities. Thus, the constrained OCP is turned into an unconstrained OCP, which yields a standard BVP of differential–algebraic equations arising from the calculus of variations. One advantage of the approach is that the solution strictly stays inside the constraints and that no knowledge of the optimal switching structure and interior boundary conditions are required.

The approach seems to be of broad applicability as it can handle a collection of constraints, provided that they have distinct orders. This condition is necessary in order to "differentially separate" the constraints, which is illustrated for the Goddard problem in Section 5 by successively incorporating the constraints.

Ongoing research concerns the proof of convergence towards the optimal solution for decreasing penalty parameters $\varepsilon \to 0$ as well as the generalization and formalization of the saturation function approach to nonlinear systems with constraints of distinct order. First steps into this direction can be found in (Graichen, 2006) in the context of feedforward control design with constraints on the input, output, and a finite number of its time derivatives.

## REFERENCES

U.M. Ascher, R.M.M. Mattheij, and R.D. Russell. *Numerical solution of boundary value problems of ordinary differential equations.* Prentice Hall, 1988.

A.E. Bryson. *Dynamic Optimization.* Addison–Wesley, Menlo Park, CA, 1999.

A.E. Bryson and Y.-C. Ho. *Applied Optimal Control.* Ginn & Company, Waltham, Massachusetts, 1969.

B. Garfinkel. A solution of the Goddard problem. *SIAM J. Contr.*, 1:349–368, 1963.

R.H. Goddard. A method for reaching extreme altitudes. *Smithsonian Int. Misc. Collections 71*, 1919.

K. Graichen. *Feedforward Control Design for Finite–Time Transition Problems of Nonlinear Systems with Input and Output Constraints.* Doctoral Thesis, Universität Stuttgart. Shaker, Aachen (Germany), 2006. http://elib.uni-stuttgart.de/opus/volltexte/2007/3004.

M. Milam. *Real–time optimal trajectory generation for constrained dynamical systems.* PhD thesis, California Institute of Technology, Pasadena, CA, 2003.

H. Munick. Goddard problem with bounded thrust. *AIAA Journal*, 3:1283–1285, 1965.

R. Pytlak. *Numerical Methods for Optimal Control Problems with State Constraints.* Springer, Berlin, Germany, 1999.

H. Seywald. Trajectory optimization based on differential inclusion. *J. Guid. Contr. Dyn.*, 17:480–487, 1994.

H. Seywald and E.M. Cliff. Goddard problem in presence of a dynamic pressure limit. *J. Guid. Contr. Dyn.*, 16, 1992.

L.F. Shampine, J. Kierzenka, and M.W. Reichelt. Solving boundary value problems for ordinary differential equations in MATLAB with bvp4c. http://www.mathworks.com/bvp_tutorial, 2000.

P. Tsiotras and H.J. Kelley. Goddard problem with constrained time of flight. *J. Guid. Contr. Dyn.*, 15:289–296, 1992.